


# Effect of the quenching residual stress on ductile fracture behavior of pre-stretched aluminum alloy plates

Huafeng Ding<sup>1,2</sup>  · Caichao Zhu<sup>2</sup> · Chaosheng Song<sup>2</sup> · Dong Qian<sup>3</sup>

Received: 22 August 2015 / Accepted: 7 January 2017  
© The Brazilian Society of Mechanical Sciences and Engineering 2017

**Abstract** The aim of this study is to investigate the effect of quenching residual stress on the ductile fracture behavior of pre-stretched 7075 aluminum alloy plate. The GTN ductile fracture model is adopted for the failure analysis and implemented in the finite element package ABAQUS. Five cases of plates with different thicknesses are selected to study the effect of the quenching residual stress. By monitoring the average stress triaxialities at the surface and the central part of the plate, a new equation describing the relationship between the equivalent strains to fracture and the average stress triaxiality is proposed. Results show that the average stress triaxiality was strongly influenced by the quenching residual stress. The thicker the plate, the higher was the value of the average stress triaxiality at the central part of the plate and, as a result, the easier the crack occurs.

**Keywords** Aluminum alloy plate · Pre-stretching process · Quenching residual stress · Ductile fracture · Average stress triaxiality

## List of symbols

$B$  Void nucleation coefficient  
 $f$  Void volume fraction

$f_c$	Critical void volume fraction at the onset of coalescence
$f_f$	Critical void volume fraction at the onset of fracture
$f_n$	Total void volume fraction that can be nucleated
$f^*(f)$	Void volume fraction function
$\mathbf{I}$	Unit tensor
$q_1, q_2, q_3$	Parameters for the GTN model
$S_n$	Standard deviation of the distribution of the plastic strain for void nucleation
$\Delta f$	Increment of void volume fraction
$\Delta f_{\text{growth}}$	Increment of void volume fraction for the growth of existing voids
$\Delta f_{\text{nucleation}}$	Increment of void volume new fraction for the nucleation of voids
$\Delta \mathbf{e}^p$	Increment of plastic strain tensor
$\Delta \bar{\varepsilon}^p$	Increment of equivalent plastic strain
$\varepsilon_n$	Mean value of the distribution of the plastic strain for void nucleation
$\bar{\varepsilon}$	Equivalent strain
$\bar{\varepsilon}_f$	Equivalent strain to fracture
$\left(\sigma_h/\sigma_{eq}\right)_{av}$	Yield function
$\sigma_{eq}$	Mises equivalent stress
$\sigma_h$	Hypostatic stress
$\sigma_y$	Yield stress
$\sigma_h/\sigma_{eq}$	Stress triaxiality
$\left(\sigma_h/\sigma_{eq}\right)_{av}$	Average stress triaxiality

Technical editor: Eduardo Alberto Fancello.

✉ Caichao Zhu  
cczhu@cqu.edu.cn

<sup>1</sup> School of Mechanical and Automotive Engineering, Hubei University of Arts and Science, Hubei 441053, China

<sup>2</sup> The State Key Laboratory of Mechanical Transmissions, Chongqing University, Chongqing 400030, China

<sup>3</sup> Department of Mechanical Engineering, University of Texas at Dallas, Richardson, TX 75080, USA

## 1 Introduction

Wide applications of high-strength aluminum alloys in many industries such as aerospace and automotive have led to a growing need for understanding their mechanical

properties. In many of these applications, the aluminum alloy needs to be processed by rolling, quenching and stretching [1]. The quenching process is known to improve the material mechanical property. However, it also induces a high amount of residual stress, which cannot be thermally relieved while maintaining the alloy's high mechanical properties [2]. Generally, the quench-induced stresses can be relieved by applying plastic strain in the rolling direction. In this process, however, the aluminum alloy plate may be subjected to ductile fracture. For a plate with large dimensions, the sudden drop in the applied load due to the fracture process poses a threat to the service life of the stretching machines. As such, a study of the mechanism of ductile fracture for quenched aluminum alloy plate under stretch is not only of fundamental interest, but also of practical importance in terms of designing the stretching process.

The fracture of aluminum alloy plate under the stretching process can be considered as a ductile type of failure and a significant amount of work has been published. Physical observation and micromechanical analysis have led to the development of a number of phenomenological or micro/meso-mechanical models for the prediction of ductile fracture initiation [3–6]. Among those models, the model proposed by Gurson [7] based on a continuum-mechanics framework has received considerable attention, and it was applied to simulate the ductile fracture of metals with the modification by Tvergaard [8] and Needleman [9] to describe the nucleation, growth and coalescence of voids in the materials, which is known as the GTN model. McClintock [10] and Rice and Tracey [11] have shown that the ductile fracture is strongly dependent on hydrostatic stress. Atkins [12] also pointed out that the criteria for fracture initiation should be dependent on hydrostatic stress. The stress triaxiality, which is defined as the ratio of the hydrostatic stress and the von Mises equivalent stress, is an important factor that controls the initiation of ductile fracture. To study the entire ductile fracture behavior, Bao and Wierzbicki [13] introduced the concept of the average stress triaxiality. The average stress triaxiality is defined as

$$\left(\frac{\sigma_h}{\sigma_{eq}}\right)_{av} = \frac{1}{\bar{\epsilon}_f} \int_0^{\bar{\epsilon}_f} \frac{\sigma_h}{\sigma_{eq}} d\bar{\epsilon}, \quad (1)$$

where  $\sigma_h$  denotes the hydrostatic stress,  $\sigma_{eq}$  represents Mises equivalent stress,  $\sigma_h/\sigma_{eq}$  and  $\left(\sigma_h/\sigma_{eq}\right)_{av}$  represent stress triaxiality and average stress triaxiality, respectively,  $\bar{\epsilon}$  is equivalent strain and  $\bar{\epsilon}_f$  is equivalent strain to fracture. Bao and Wierzbicki [13, 14] have also observed that the mechanism of ductile fracture is different depending on the amount of triaxiality and they investigated a wide range of stress triaxiality for the fracture ductility of 2024-T351 aluminum alloy. Zhou et al. [15] studied the ductile

fracture behaviors of 5083 aluminum alloy including the residual stress effect through a series of experiments and finite element analyses, and the results indicated that the residual stress has a significant effect on ductile fracture resistance. Farahani and Sattari-Far [16] investigated the effects of residual stresses on crack behavior and showed that the crack driving forces and the crack-tip stress field were distinctly affected by residual stress. For a pre-stretched aluminum alloy plate, Ding et al. [17] studied the variations of elliptical cracks considering the effect of quenching residual stress and results show that the cracks' propagation is affected significantly by the quenching residual stress. During the entire stretching process, the stress is affected by the quenching residual stress; however, there is little literature on the study of fracture behavior considering the effect of quenching residual stress.

In this paper, the effect of quenching residual stress on the fracture behavior during the stretching process was investigated for 7075 aluminum alloy plates. Five cases of 7075 plates with different thicknesses are selected in the study. The GTN ductile fracture model is used in the finite element package ABAQUS [18], and the quenching residual stresses are input in the model as the initial stresses. The stretching process is simulated until fracture occurs. The stress states in the plates are calculated with which the stress triaxiality is derived to study its effect on the equivalent strain to fracture. By monitoring the average stress triaxialities at the central part of the plate, a new equation describing the relationship between the equivalent strain to fracture and the average stress triaxiality is proposed.

## 2 Pre-stretching fracture model for aluminum alloy plate

### 2.1 Ductile fracture model

Since Gurson developed the ductile fracture model for a voided material in 1977 [7], numerous investigations have been done based on the Gurson model, which has demonstrated that it is a key advantage of simulation of ductile fracture, especially the model modified by Tvergaard with respect to the yield condition and damage evolution and by Needleman to introduce the law of void nucleation, which is called Gurson–Tvergaard–Needleman (GTN) model. The constitutive equation of the GTN model is expressed as [8, 9]:

$$\Phi = \left(\frac{\sigma_{eq}}{\sigma_y}\right)^2 + 2q_1 f^*(f) \cosh\left(\frac{3q_2 \sigma_h}{2\sigma_y}\right) - (1 + q_3 f^*(f)^2), \quad (2)$$

where  $\sigma_y$  represents the yield strength of the matrix,  $q_1$ ,  $q_2$  and  $q_3$  are the constitutive parameters with  $q_3 = q_1^2$ ,

and  $f^*(f)$  is a function of the void volume fraction  $f$  by taking into account the accelerated process of coalescence after reaching a critical void volume fraction  $f_c$ . This function is defined by:

$$f^*(f) = \begin{cases} f, & f \leq f_c \\ f_c + \frac{1/q_1 - f_c}{f_f - f_c} (f - f_c), & f_c < f \leq f_f \end{cases}, \quad (3)$$

where  $f_f$  is the void volume fraction at the fracture. The void coalescence is considered to take place when the void volume fraction reaches a critical value  $f_c$  and the material fractures when the void volume fraction reaches  $f_f$ .

In general, the evolution of the void volume fraction is driven by the growth of existing voids and the nucleation of new voids:

$$\Delta f = \Delta f_{\text{growth}} + \Delta f_{\text{nucleation}}. \quad (4)$$

Void growth can be expressed by volumetric expansion in mesoscale:

$$\Delta f_{\text{growth}} = (1 - f) \Delta \epsilon^p : \mathbf{I}, \quad (5)$$

where  $\Delta \epsilon^p$  is the increment of the plastic strain tensor and  $\mathbf{I}$  denotes the tensor. Here, we consider the plastic strain controlled nucleation, so that void nucleation can be written as follows:

$$\Delta f_{\text{nucleation}} = B \Delta \bar{\epsilon}^p, \quad (6)$$

where  $\Delta \bar{\epsilon}^p$  is the increment of equivalent plastic strain and the parameter  $B$  is chosen so that void nucleation follows a normal distribution around a critical, which was introduced by Needleman [8]:

$$B = \frac{f_n}{s_n \sqrt{2\pi}} \exp \left[ -\frac{1}{2} \left( \frac{\bar{\epsilon}^p - \epsilon_n}{s_n} \right)^2 \right]. \quad (7)$$

Here,  $f_n$  is the void volume fraction of void nucleating particles,  $s_n$  is the standard deviation and  $\epsilon_n$  is the mean nucleating strain.

## 2.2 Material parameters and boundary condition

Due to the high mechanical properties like high yield strength and high toughness, etc., aluminum 7075 alloys are widely used in aerospace structures and automobile components [19], and hence the 7075 aluminum alloy is selected for the study as shown in Fig. 1. The 7075 aluminum alloy may be modeled using an isotropic plastic model (J2-plasticity) and isotropic hardening, while the hardening behavior is obtained from the experimental curve in the study of Brar et al. [19]. There are ten parameters for GTN model, which are adopted from Refs. [19, 20], as shown in Table 1.

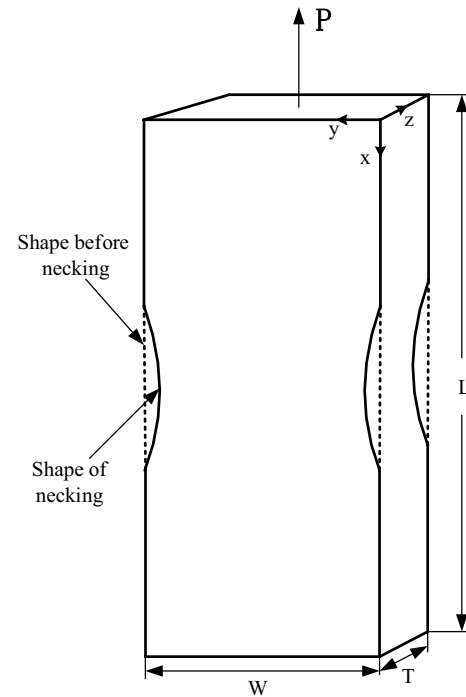


**Fig. 1** Pre-stretched aluminum alloy plate

**Table 1** Material parameters of the 7075 aluminum alloy

Young's modulus (GPa)	71.7
Poisson's ratio	0.33
Yield strength (MPa)	546
Density (kg/m <sup>3</sup> )	2810
$q_1$	1
$q_2$	1.5
$f_n$	0.01
$s_n$	0.1
$\epsilon_n$	0.3
$f_0$	0.0001
$f_c$	0.15
$f_f$	0.25

All the simulations were carried out using the commercial finite element package ABAQUS to obtain individual components of stress and strain tensors at the fracture location. Eight-node linear brick elements with reduced Gaussian integration and hourglass control (C3D8R in ABAQUS Explicit) were used. In the actual production, after the quenching process, the aluminum alloy plate will be stretched by stretching machine to relieve the residual stress. So, in the finite element model, one side of the plate was fixed as the plate clamped in practical and the other side was subjected to uniaxial tensile loading until failure, and the quenching residual stress was simulated [21, 22] and

**Table 2** Dimensions of aluminum alloy plate

No.	Dimensions of plates (length $\times$ width $\times$ thickness)/mm
1	10,000 $\times$ 1500 $\times$ 40
2	10,000 $\times$ 1500 $\times$ 80
3	10,000 $\times$ 1500 $\times$ 120
4	10,000 $\times$ 1500 $\times$ 160
5	10,000 $\times$ 1500 $\times$ 200

imported into the finite element model as the initial stress state. The residual stress after quenching might be over 200 MPa, and the thicker the plate, the larger is the quenching residual stress. The shear stress in quenched plates and the stress in the thickness direction can be neglected since they are very small compared to the stresses in length and width direction. Five cases of plates with different thicknesses, i.e., 40, 80, 120, 160, and 200 mm, are selected to investigate the effect of quenching residual stress on the fracture behavior, with the dimensions listed in Table 2. Residual stresses in the thick direction, i.e., the Z direction, are shown in Fig. 2. The pattern of the distribution of the quenching residual stresses of plates with different thicknesses seems to be similar.

### 3 Results and discussions

#### 3.1 Fracture process simulation with pre-stretched plates

The models are developed with the commercial finite element package ABAQUS. Take a plate of 120 mm thickness for example. Figure 3 shows the distributions of the stress and strain as the fracture occurs. It can be seen that the contraction before fracture causes the concentration of the stress, which represents the triaxial stress state. The stresses far away from the fracture zone distribute evenly

and represent the uniaxial stress state. The plastic strain at the central part of the fracture zone is most significant, where the crack occurs initially.

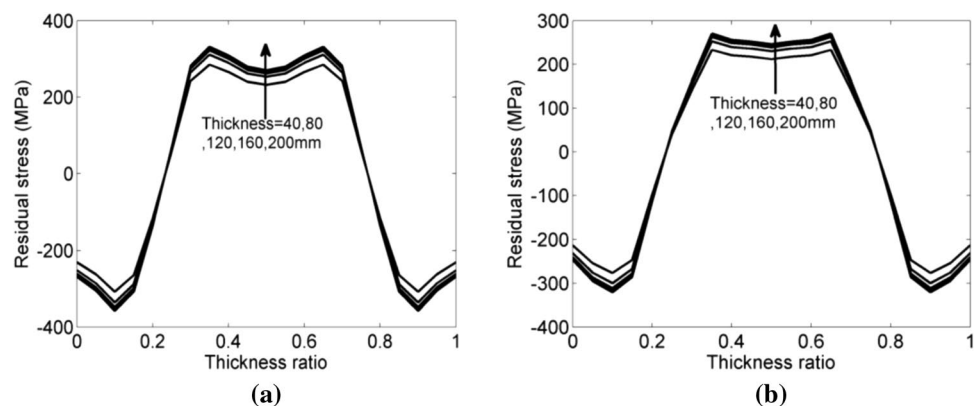
Figure 4 shows the comparison of the current results with and without the residual stress and the experimental results from Refs. [19, 23]. It can be seen that the simulation without the effect of quenching residual stress matches very well with the experimental result. The quenching residual stress affects the yield stress of the material, but has little effect on the flow stress and the strain to the fracture. For the entire deformation, the components of stress and strain tensors will be affected by the quenching residual stress. This effect will be simulated by the GTN model with the parameters selected.

#### 3.2 Effects of the quenching residual stress

Since the above correlation of the experimental and numerical results is almost perfect, it is reasonable to study the fracture ductility based on the individual components of stress and strain tensors at locations of fracture initiation obtained from numerical simulations. The numerical simulation results are shown in Fig. 5.

Figure 5 indicates that the engineering stress–strain relationships of different plates are similar, and as the thickness of the plate increases the final equivalent strain to the fracture only decreases slightly. This is because the quenching residual stress distributes evenly in the global scale. However, the ductile fracture is mainly influenced by the local stress state, for example the stress triaxiality. The effects of quenching residual stress on the stress triaxiality in the entire deformation process are shown in Fig. 6, from which it can see that the quenching residual stress has significant effects on stress triaxialities. As the stretching process goes on, the stress triaxiality at the surface increases to 1/3 from a negative value, then remains constant for a while and finally increases again. The quenching residual stresses at the surface are compressive stresses, which explain why the initial stress triaxiality is negative. As the load increases,

**Fig. 2** Distribution of quenching residual stress. **a** Residual stress in X direction. **b** Residual stress in Y direction



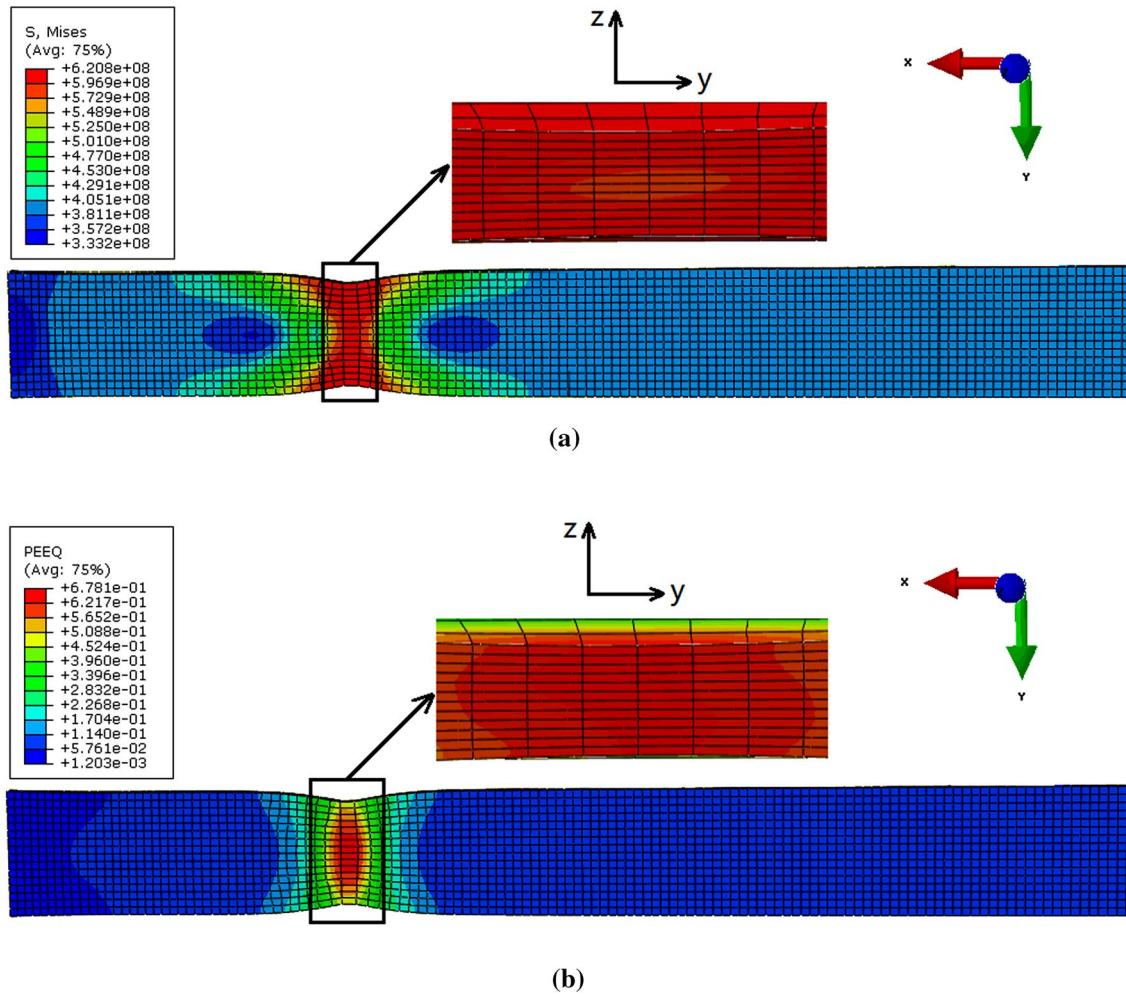


**Fig. 3** Distributions of stress and strain for the aluminum alloy plate. **a** The distribution of Mises equivalent stress. **b** The distribution of equivalent strain

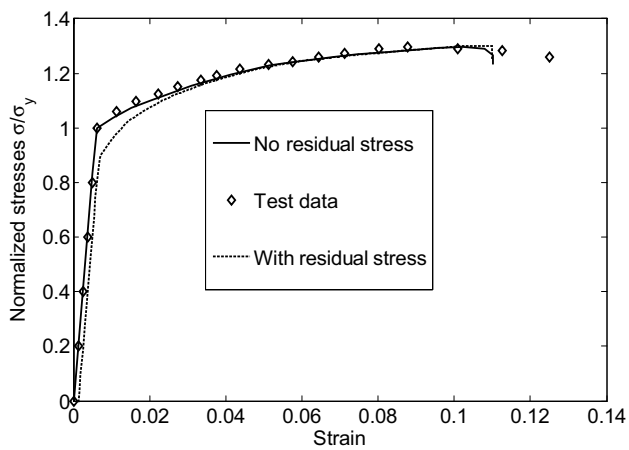


**Fig. 4** Comparison of true stress–strain curve between test data and simulations

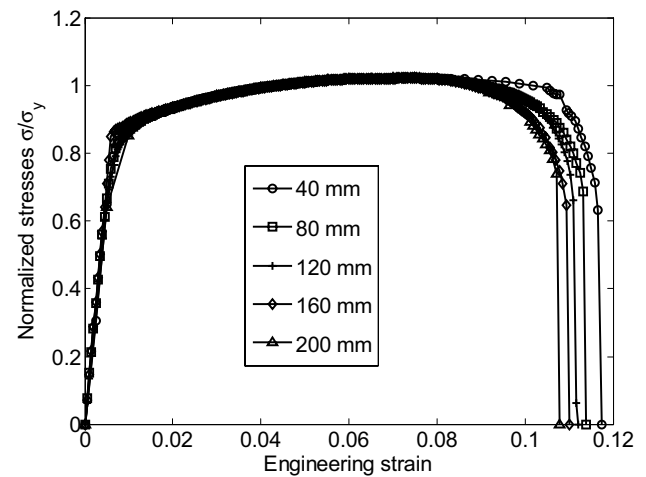


**Fig. 5** The engineering stress–strain curve



**Fig. 6** The effects of quenching residual stress on stress triaxiality. **a** Stress triaxialities at the surface. **b** Stress triaxialities at the center

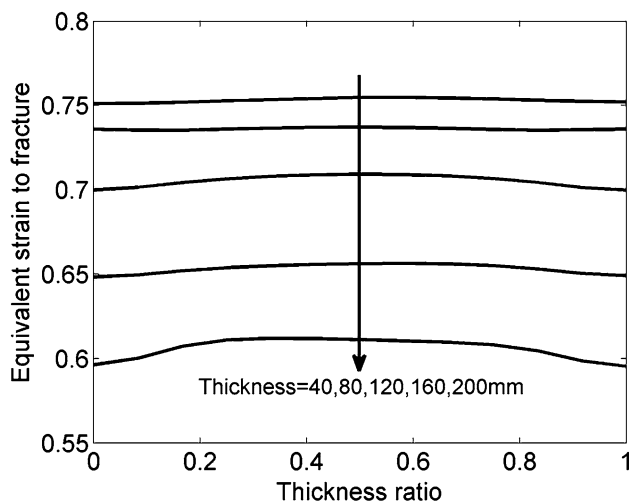
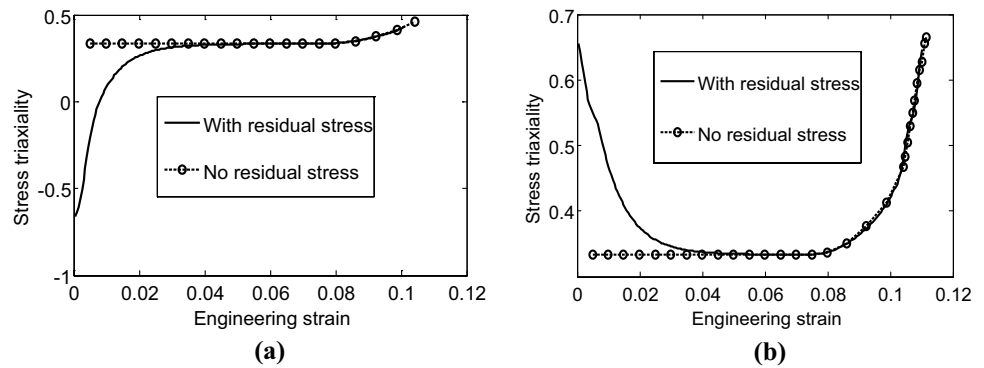


**Fig. 7** Distributions of equivalent strain to fracture along the Z direction

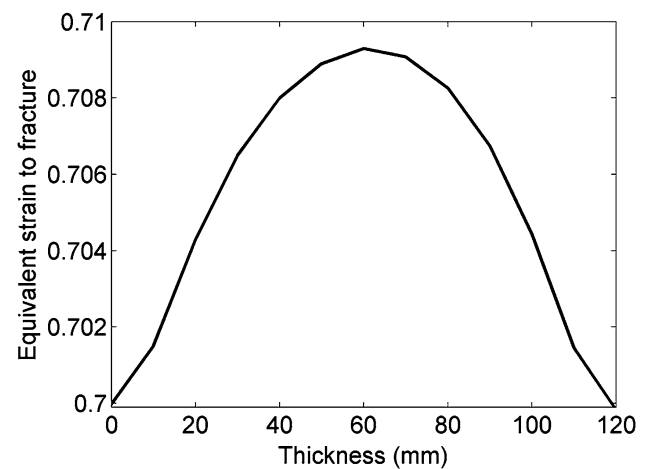


**Fig. 8** Distribution of equivalent strain to fracture for the 120 mm plate

the quenching residual stresses inside the plate are eliminated, which turns the state into a uniaxial stress state, i.e., with a  $1/3$  stress triaxiality. As the plastic deformation occurs, the plate starts contracting locally, which means that the stress triaxiality increases again. While for the central position of the plates, the quenching residual stresses at this area represents the tensile state and the stress triaxiality value is high initially. As the load increases, the values of the stress triaxiality at the central area decreases, until the uniaxial stress states occur. Once the plate starts contracting, the stress triaxiality increases again.

The equivalent strains to fracture along the thickness direction are calculated in the simulation, which are shown in Fig. 7. It can be seen clearly that the equivalent strains to fracture decrease quickly as the thicknesses of the plates increase, and for each case the equivalent strain to fracture varies with the thickness. To see the variation between the equivalent strain to fracture and the thickness of the plate, the case of the 120 mm-thick plate is shown in Fig. 8, which shows that the equivalent strain to fracture distributes

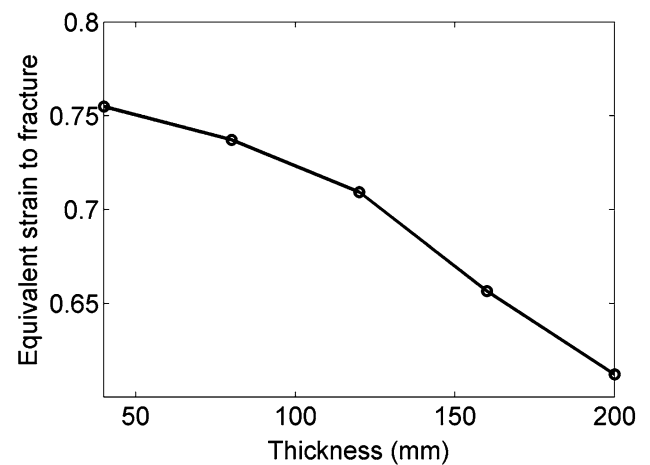


**Fig. 9** Equivalent strains to fracture at the central part of the aluminum alloy plates

symmetrically along the central plane, with the largest value occurring at the central position. This means that the crack would generate initially from the central position.

**Fig. 10** Stress triaxialities at the surface and central part of different plates. **a** Stress triaxialities at the surface. **b** Stress triaxialities at the center

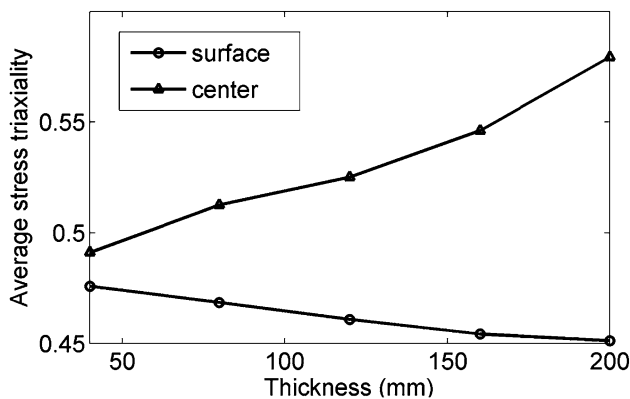
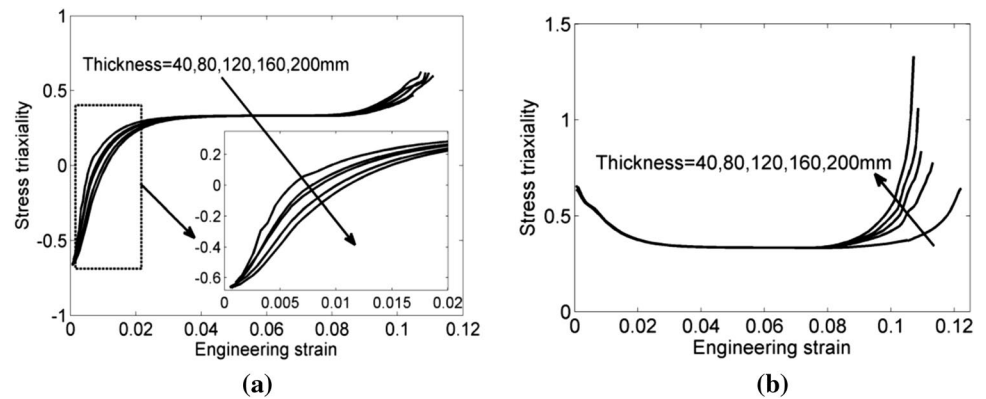


**Fig. 11** Average stress triaxialities at the surface and center part of the plates

The equivalent strains to fracture at the central position play an extremely important role in the initiation of fracture. Figure 9 shows the variation of equivalent strains to fracture with the thickness. As the thickness of the plate increases, the largest equivalent strain to fracture at the central position decreases. This indicates that if the plates are stretched up to the same level of plastic strain, the thicker plates are more prone to fracture.

The stress triaxialities as the plate fractures are calculated through the stress components. Figure 10 shows the stress triaxialities at the surface and the central position of the plates. It can be seen that the amplitudes of stress triaxialities at the surface decrease as the thickness of the aluminum alloy plates increase before the uniaxial state of stress; on the other hand, the amplitudes of stress triaxialities at the center increase as the thickness of the aluminum alloy plates increase at the initial fracture.

Generally, the stress triaxiality varies during the deformation process of the materials, as shown in Fig. 10, which makes it difficult to analyze the ductile fracture. The average stress triaxialities at the surface and central part of five cases for aluminum alloy plates with different thicknesses are calculated, as shown in Fig. 11.

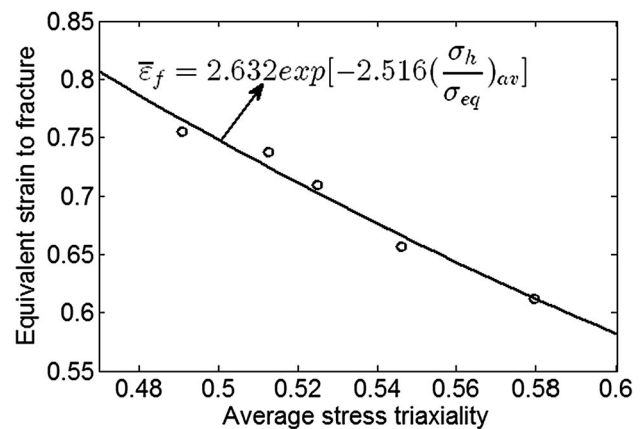


**Fig. 12** Relationship between equivalent strain to fracture and average stress triaxiality

It can be seen that the average stress triaxiality at each position is above 0.4. For a single plate, the average stress triaxiality at the central area is larger than the one at the surface. As the thickness of the plates increases, the differences between the surface and the central area become more significant, and while the average stress triaxiality at the central area increases, the average stress triaxiality at the surface decreases. Results shown in Fig. 11 indicate that the thicker the plate, the easier does the crack occur. The quenching residual stress at the surface in the compressive state would inhibit the generation of the crack, while the quenching residual stress at the central area represents the tensile state which would facilitate the generation of the crack. The thicker the plate, the higher is the amplitude of the quenching residual stress and the more significant is of the effect on the initiation and inhabitation of the crack.

The initiation of the crack is related to the average stress triaxiality. To predict the fracture initiation at the central area of the plate during the stretching process, the relationship of the equivalent strain and the average stress triaxiality is calculated, which is shown in Fig. 12. The results are fitted to derive a new equation describing the relationship

between the equivalent strain to the fracture and the average stress triaxiality:

$$\bar{\epsilon}_f = 2.632 \exp \left\{ -2.516 \left( \frac{\sigma_h}{\sigma_{eq}} \right)_{av} \right\}. \quad (8)$$

The equation above is also described in Fig. 12. The initiations of fracture for the 7075 aluminum alloy plates with different thicknesses can be obtained easily according to Figs. 11 and 12. So the equation is believed to be a useful tool for the prediction of fracture initiation of aluminum alloy plate with quenching residual stress during the stretching process, and to prevent the fracture of the plate, the stretching process for the 7075 aluminum alloy plate also can be designed based on this equation.

## 4 Conclusions

The fracture during the stretching process will pose a threat to the service life of the stretching machines; to predict the fracture and protect the machines, the effect of quenching residual stress on the ductile fracture behavior of a 7075 aluminum alloy plate is investigated. Five cases of plates with different thicknesses are selected to study the effect of the quenching residual stress, and the entire deformations of the plates are simulated to get the components of stresses and strains. With the effect of residual stress, the variations of stress triaxialities at the surface and the central part of the plates are calculated, and the average stress triaxialities during the deformation are also obtained, based upon which a new equation describing the relationship between the equivalent strain to fracture and the average stress triaxiality is proposed. This is believed to be a useful tool for the prediction of fracture initiation of aluminum alloy plate with quenching residual stress during the stretching process. By analyzing the calculated results of example cases, the following specific conclusions can be obtained:

1. A new equation describing the relationship between the equivalent strain to fracture and the average stress triaxiality is proposed, by which the initiation of fracture of aluminum alloy plate can be predicted. It can be used to design the stretching process to protect the fracture of the plate.
2. Before the fracture of the plate, the states transform from the uniaxial stress state to the multiaxial stress state. The equivalent strain to fracture distributes symmetrically along the central plane of the plate, and the largest value occurs at the central position. With the increase of the plate thickness, the largest equivalent

strain to fracture at the central position decreases. It indicates that the initiation of fracture will occur at the central position of the plate, and the thicker plate is more prone to fracture.

3. During the entire deformation, the stress triaxialities at the surface and center of the plate are calculated. With the effect of the quenching residual stress, the values of the stress triaxialities reach 1/3 from a negative and positive value, respectively. This state will affect the average stress triaxialities for the entire deformation.

**Acknowledgements** The authors appreciate the financial support from the National Major Scientific and Technological Special Project (2015ZX04005-011).

## References

1. Koç M, Culp J, Altan T (2006) Prediction of residual stresses in quenched aluminum blocks and their reduction through cold working processes. *J Mater Process Technol* 174(1–3):342–354. doi:[10.1016/j.jmatprotec.2006.02.007](https://doi.org/10.1016/j.jmatprotec.2006.02.007)
2. Tanner DA, Robinson JS (2003) Modelling stress reduction techniques of cold compression and stretching in wrought aluminium alloy products. *Finite Elem Anal Des* 39(5–6):369–386. doi:[10.1016/S0168-874X\(02\)00079-3](https://doi.org/10.1016/S0168-874X(02)00079-3)
3. Andrade Pires FM, de Souza Neto EA, Owen DRJ (2004) On the finite element prediction of damage growth and fracture initiation in finitely deforming ductile materials. *Comput Methods Appl Mech Eng* 193(48–51):5223–5256. doi:[10.1016/j.cma.2004.01.038](https://doi.org/10.1016/j.cma.2004.01.038)
4. Bai Y, Wierzbicki T (2008) A new model of metal plasticity and fracture with pressure and Lode dependence. *Int J Plast* 24(6):1071–1096. doi:[10.1016/j.ijplas.2007.09.004](https://doi.org/10.1016/j.ijplas.2007.09.004)
5. Benseddig N, Imad A (2008) A ductile fracture analysis using a local damage model. *Int J Press Vessels Pip* 85(4):219–227. doi:[10.1016/j.ijvp.2007.09.003](https://doi.org/10.1016/j.ijvp.2007.09.003)
6. Li H, Fu MW, Lu J, Yang H (2011) Ductile fracture: experiments and computations. *Int J Plast* 27(2):147–180. doi:[10.1016/j.ijplas.2010.04.001](https://doi.org/10.1016/j.ijplas.2010.04.001)
7. Gurson AL (1977) Continuum theory of ductile rupture by Void nucleation and growth: part I—yield criteria and flow rules for porous ductile media. *J Eng Mater Technol* 99(1):2–15. doi:[10.1115/1.3443401](https://doi.org/10.1115/1.3443401)
8. Chu CC, Needleman A (1980) Void nucleation effects in biaxially stretched sheets. *J Eng Mater Technol* 102(3):249–256. doi:[10.1115/1.3224807](https://doi.org/10.1115/1.3224807)
9. Tvergaard V (1989) Material failure by void growth to coalescence. In: John WH, Theodore YW (eds) *Advances in applied mechanics*, vol 27. Elsevier, pp 83–151. doi: [10.1016/S0065-2156\(08\)70195-9](https://doi.org/10.1016/S0065-2156(08)70195-9)
10. McClintock FA (1968) A criterion for ductile fracture by the growth of holes. *J Appl Mech* 35(2):363–371. doi:[10.1115/1.3601204](https://doi.org/10.1115/1.3601204)
11. Rice JR, Tracey DM (1969) On the ductile enlargement of voids in triaxial stress fields. *J Mech Phys Solids* 17(3):201–217. doi:[10.1016/0022-5096\(69\)90033-7](https://doi.org/10.1016/0022-5096(69)90033-7)
12. Atkins AG (1996) Fracture in forming. *J Mater Process Technol* 56(1–4):609–618. doi:[10.1016/0924-0136\(95\)01875-1](https://doi.org/10.1016/0924-0136(95)01875-1)
13. Bao Y, Wierzbicki T (2004) On fracture locus in the equivalent strain and stress triaxiality space. *Int J Mech Sci* 46(1):81–98. doi:[10.1016/j.ijmecsci.2004.02.006](https://doi.org/10.1016/j.ijmecsci.2004.02.006)



14. Bao Y, Wierzbicki T (2004) A comparative study on various ductile crack formation criteria. *J Eng Mater Technol* 126(3):314–324. doi:[10.1115/1.1755244](https://doi.org/10.1115/1.1755244)
15. Zhou J, Gao X, Hayden M, Joyce JA (2012) Modeling the ductile fracture behavior of an aluminum alloy 5083-H116 including the residual stress effect. *Eng Fract Mech* 85:103–116. doi:[10.1016/j.engfracmech.2012.02.014](https://doi.org/10.1016/j.engfracmech.2012.02.014)
16. Farahani M, Sattari-Far I (2011) Effects of residual stresses on crack-tip constraints. *Sci Iran* 18(6):1267–1276. doi:[10.1016/j.scient.2011.11.024](https://doi.org/10.1016/j.scient.2011.11.024)
17. Ding H-F, Zhu C-C, Li D-F, Du X-S, Liu M-Y (2012) Mode I stress intensity factor calculation of elliptical cracks in aluminum alloy thick plates considering quenching residual stress. *Zhongguo YOUSE Jinshu Xuebao/Chin J Nonferrous Metals* 22(12):3320–3326
18. Hibbitt HD, Karlsson BI, Sorensen EP (2011) ABAQUS theory manual-version 6.11 Edition. Theory manual-version 6.11 Edition. HKS Inc, Pawtucket, USA
19. Brar NS, Joshi VS, Harris BW, Elert M, Furnish MD, Anderson WW, Proud WG, Butler WT (2009) Constitutive model constants for Al7075-T651 and Al7075-T6. Paper presented at the shock compression of condensed matter - 2009, Tennessee, USA
20. Chen Y, Ghosh S (2012) Micromechanical analysis of strain rate-dependent deformation and failure in composite microstructures under dynamic loading conditions. *Int J Plast* 32–33:218–247. doi:[10.1016/j.ijplas.2011.10.008](https://doi.org/10.1016/j.ijplas.2011.10.008)
21. C-c Z, J-y L (2012) Stretch rate and deformation for pre-stretching aluminum alloy sheet. *J Cent South Univ Technol* 19(4):875–881. doi:[10.1007/s11771-012-1086-2](https://doi.org/10.1007/s11771-012-1086-2)
22. Zhu C, Luo J, Li D, Zhong Y, Li Y (2010) Numerical simulation and experimental investigation of the aluminum alloy quenching-induced residual stress by considering the flow stress characteristic. *Jixie Gongcheng Xuebao/J Mech Eng* 46(22):41–46. doi:[10.3901/jme.2010.22.041](https://doi.org/10.3901/jme.2010.22.041)
23. Jordon JB, Horstemeyer MF, Solanki K, Bernard JD, Berry JT, Williams TN (2009) Damage characterization and modeling of a 7075-T651 aluminum plate. *Mater Sci Eng A* 527(1–2):169–178. doi:[10.1016/j.msea.2009.07.049](https://doi.org/10.1016/j.msea.2009.07.049)